





Mechanistic insights into the interaction of the MOG1 protein with the cardiac sodium channel Na_v1.5 clarify the molecular basis of Brugada syndrome

Received for publication, May 21, 2018, and in revised form, September 23, 2018. Published, Papers in Press, October 3, 2018, DOI 10.1074/jbc.RA118.003997

Gang Yu^{‡§}, Yinan Liu[‡], Jun Qin[§], Zhijie Wang^{‡§}, Yushuang Hu[‡],  Fan Wang[§], Yabo Li^{§¶}, Susmita Chakrabarti[§], Qiuyun Chen^{§1}, and  Qing Kenneth Wang^{‡§||2}

From the [‡]Key Laboratory of Molecular Biophysics of the Ministry of Education, Cardio-X Center, College of Life Science and Technology and Center for Human Genome Research, Huazhong University of Science and Technology, Wuhan 430074, China, [§]Center for Cardiovascular Genetics, Department of Molecular Cardiology, Lerner Research Institute, Cleveland Clinic; Department of Molecular Medicine, Cleveland Clinic Lerner College of Medicine, Case Western Reserve University, Cleveland, Ohio 44195, [¶]College of Life Sciences, Lanzhou University, Lanzhou, Gansu, China, and ^{||}Department of Genetics and Genome Sciences, Case Western Reserve University School of Medicine, Cleveland, Ohio 44106

Edited by Mike Shipston

Na_v1.5 is the α -subunit of the cardiac sodium channel complex. Abnormal expression of Na_v1.5 on the cell surface because of mutations that disrupt Na_v1.5 trafficking causes Brugada syndrome (BrS), sick sinus syndrome (SSS), cardiac conduction disease, dilated cardiomyopathy, and sudden infant death syndrome. We and others previously reported that Ran-binding protein MOG1 (MOG1), a small protein that interacts with Na_v1.5, promotes Na_v1.5 intracellular trafficking to plasma membranes and that a substitution in MOG1, E83D, causes BrS. However, the molecular basis for the MOG1/Nav1.5 interaction and how the E83D substitution causes BrS remains unknown. Here, we assessed the effects of defined MOG1 deletions and alanine-scanning substitutions on MOG1's interaction with Na_v1.5. Large deletion analysis mapped the MOG1 domain required for the interaction with Na_v1.5 to the region spanning amino acids 146–174, and a refined deletion analysis further narrowed this domain to amino acids 146–155. Site-directed mutagenesis further revealed that Asp-148, Arg-150, and Ser-151 cluster in a peptide loop essential for binding to Na_v1.5. GST pulldown and electrophysiological analyses disclosed that the substitutions E83D, D148Q, R150Q, and S151Q disrupt MOG1's interaction with Na_v1.5 and significantly reduce its trafficking to the cell surface. Examination of MOG1's 3D structure revealed that Glu-83 and the loop containing Asp-148, Arg-150, and Ser-151 are spatially proximal, suggesting that these residues form a critical binding site for Na_v1.5. In conclusion,

our findings identify the structural elements in MOG1 that are crucial for its interaction with Na_v1.5 and improve our understanding of how the E83D substitution causes BrS.

Cardiac arrhythmias cause more than 300,000 sudden deaths each year in the United States alone (1). Mutations in the *SCN5A* gene cause inherited cardiac arrhythmias, including Brugada syndrome (BrS)³, sick sinus syndrome (SSS), cardiac conduction disease, atrial fibrillation, and dilated cardiomyopathy (2–5). Abnormalities of cardiac sodium current were also observed in common cardiovascular diseases such as myocardial ischemia and heart failure, which are also associated with sudden deaths (6).

The cardiac voltage-gated sodium channel is responsible for the generation and conduction of cardiac action potential (7, 8). The cardiac sodium channel is a multiprotein complex consisting of an α -subunit of Na_v1.5 encoded by the *SCN5A* gene, β -subunits (β 1– β 4), and other accessory interacting proteins such as the chaperon MOG1 identified by our group using a yeast two-hybrid screen (9). MOG1 was initially identified as a Ran-binding protein and a guanine nucleotide release factor of Ran (10, 11). The interaction between MOG1 and Ran was shown to be required for efficient nuclear protein import (12). The X-ray crystal structure of yeast MOG1 was determined at 1.9 Å resolution (13). MOG1 has an interesting structure with a backbone formed by six-stranded antiparallel β -sheets flanked on both sides by helices (14). The solution structure of human MOG1 was determined recently by conventional NMR spectroscopy and has a sandwich-like structure with nine β -strands and four helices (15). The β 3 to β 9 form the central antiparallel β -sheets, which were packed by helices α 2 and α 4 on either side (15). The Asp-25, Arg-30, Asp-34, and Glu-37 residues of MOG1 play an important role in Ran binding and GTP release in mice (16). A recent study suggested that the Asp-27, Glu-50, Asp-70, and Glu-53 residues of human MOG1 were also involved in the MOG1–Ran interaction (15).

This study was supported by NHLBI, National Institutes of Health Grants R01 HL121358 and R01 HL126729; the National Natural Science Foundation of China Grants 81630002, 31430047, and 91439129; Hubei Province's Innovative Team Grant, 2016 Top-Notch Innovative Talent Development Project from the Bureau of Human Resources and Social Security of Wuhan City, Hubei Province Natural Science Programs 2016CFB224 and 2014CFA074; and Chinese National Basic Research Programs (973 Programs) 2013CB531101 and 2012CB5178 01. The authors declare that they have no conflicts of interest with the contents of this article. The content is solely the responsibility of the authors and does not necessarily represent the official views of the National Institutes of Health.

¹ To whom correspondence may be addressed: 9500 Euclid Ave., Cleveland, OH 44195. Tel.: 216-444-2122; Fax: 216-636-1231; E-mail: chengq3@ccf.org.

² To whom correspondence may be addressed. E-mail: qkwang@hust.edu.cn or wangq2@ccf.org.

³ The abbreviations used are: BrS, Brugada syndrome; SSS, sick sinus syndrome; aa, amino acid; GST–Na_v1.5–LII, GST–Na_v1.5–loop II.

Defect of MOG1–Na_v1.5 interaction causes Brugada syndrome

We reported previously that MOG1 is a key component of the cardiac sodium channel complex and is required for the full function of Na_v1.5. MOG1 was identified as a protein that interacts with the cytoplasmic loop II (between domains DII and DIII) of Na_v1.5 by a yeast two-hybrid screen. MOG1 increases the density of the cardiac sodium current I_{Na} by promoting the intracellular trafficking of Na_v1.5 from the endoplasmic reticulum to the plasma membrane (9, 17). Na_v1.5 failed to be transported to cell surface and accumulated in the endoplasmic reticulum when MOG1 was knocked down in Na_v1.5/HEK cells, the HEK293 cells with stable overexpression of Na_v1.5. Overexpression of MOG1 successfully rescued the defective trafficking and reduced I_{Na} density associated with Na_v1.5 mutation D1275N causing SSS, atrial fibrillation, and dilated cardiomyopathy, and mutation G1743R causing BrS (17). Therefore, MOG1 is a potential therapy for carriers with mutant Na_v1.5 having defects in cell surface trafficking of Na_v1.5. However, the underlying molecular mechanism of how MOG1 interacts with Na_v1.5 is unknown. Interestingly, a mutation in MOG1, E83D, was identified in a patient with BrS (18). MOG1 mutation E83D was reported to be a dominant negative missense mutation that significantly reduced the density of I_{Na} (18). However, the molecular mechanism of how mutation E83D results in BrS is poorly understood.

In this study, we investigated the mechanism by which MOG1 interacts with Na_v1.5. Our data demonstrate that amino acid residues Glu-83, Asp-148, Arg-150, and Ser-151 are essential for the binding of MOG1 to Na_v1.5 to generate full-scale I_{Na} . Furthermore, amino acids Leu-138 and Leu-139 of MOG1 are required for the integrity of MOG1's structure. Moreover, we found that MOG1 mutation E83D disrupted the interaction between MOG1 and Na_v1.5, and significantly reduced intracellular trafficking of Na_v1.5 to the plasma membranes, thereby providing a novel molecular mechanism for the pathogenesis of BrS.

Results

Large deletion analysis defines the MOG1 functional domain for interaction with Na_v1.5 between amino acid residues 146 and 174

MOG1 is an evolutionarily conserved protein from yeast to humans (19). Yeast two-hybrid screening and follow-up GST pull-down and co-immunoprecipitation studies showed that MOG1 interacts with cardiac sodium channel Na_v1.5 (9). Overexpression of MOG1 in HEK293 and tsA201 cells or mouse cardiomyocytes facilitates the cell surface expression of Na_v1.5 and enhances sodium current density (9). To determine the functional domain(s) of MOG1 in enhancing Na_v1.5 cell surface expression, and thus increasing the sodium current density, we carried out a systematic deletion analysis. We created serial deletions of MOG1 from the C terminus, including deletion 1–174 aa, 1–146 aa, and 1–101 aa (Fig. 1A). The deletion mutants were then co-transfected into Na_v1.5/HEK cells with constant expression of Na_v1.5 together with pmaxEGFP. Whole-cell patch clamp recordings of selected green fluorescent cells with successful transfection of MOG1 plasmids were performed to determine the effects of MOG1 deletions on

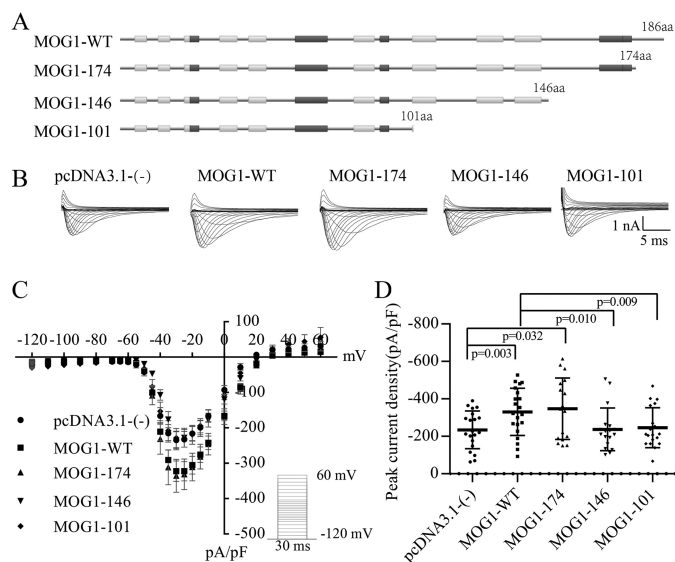


Figure 1. Large deletion analysis of MOG1 to identify the Na_v1.5 interaction domain. A, diagram (dark, alpha helix; gray, beta strand) showing WT MOG1 (MOG1-WT) and mutant MOG1 with three serial deletions from the C terminus (MOG1-174, MOG1-146, and MOG1-101). B, raw traces of sodium current recorded from Na_v1.5/HEK cells transfected with WT MOG1, each deletion mutant or vector negative control pcDNA3.1(-). C, effect of MOG1-WT and each deletion mutant on sodium current as compared with vector control. Error bars indicate S.E. D, peak sodium current density (pA/pF). The peak current density (pA/pF) was -234.49 ± 100.74 for pcDNA 3.1(-) (20 cells), -342.55 ± 117.29 for MOG1-WT (20 cells), -347.41 ± 202.50 for MOG1-174 (18 cells), -245.64 ± 106.86 for MOG1-146 (19 cells), and -237.38 ± 114.13 for MOG1-101 (18 cells). Values are mean \pm S.D.

Na_v1.5 channel function. Like the full-length WT MOG1, the first C-terminal deletion of MOG1 (1–174 aa) increased sodium current density. However, MOG1 deletions MOG1 (1–146 aa) and MOG1 (1–101 aa) failed to increase sodium current density (Fig. 1, B–D). These data suggest that amino acid residues between 146 and 174 aa are required for MOG1 to increase sodium current density.

MOG1 interacts with the cytoplasmic loop II of Na_v1.5 to facilitate its cell surface expression (9). To determine whether the MOG1 (146–174) region is involved in the interaction with Na_v1.5, GST pull-down assays were performed. GST–Na_v1.5–loop II (GST–Na_v1.5–LII) successfully pulled down the full-length MOG1 and the first C-terminal deletion mutant MOG1 (1–174) (Fig. 2, A and B). However, GST–Na_v1.5–LII failed to pull down MOG1 deletion mutants MOG1 (1–146 aa) and MOG1 (1–101 aa) (Fig. 2, A and B). These data suggest that the amino acid residues between 146 and 174 of MOG1 are involved in its interaction with the cytoplasmic loop II of Na_v1.5.

Microdeletion analysis defines the MOG1 functional domain for interaction with Na_v1.5 between amino acid residues 146 and 155

To narrow down the MOG1 functional domain for interaction with Na_v1.5, we created consecutive deletions of 10 amino acid residues for the region between amino acid residues 126 and 174 of MOG1 (Fig. 3A). The whole-cell patch clamp recordings showed that three deletion mutants, MOG1 (166–174 aa deletion), MOG1 (156–165 aa deletion), and MOG1 (126–135 aa deletion), had similar activity as WT MOG1 in

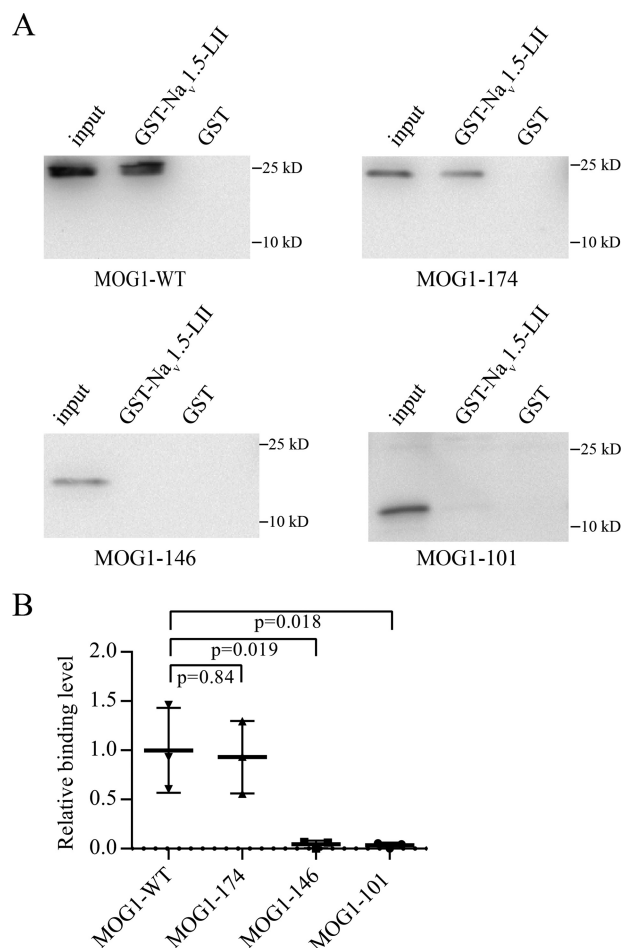


Figure 2. Interaction between WT and mutant MOG1 and Na_v1.5. A, the tsA201 cells were transfected with an expression plasmid for FLAG-tagged WT MOG1 (*MOG1-WT*) or each deletion mutant, lysed and mixed with GST–Na_v1.5–LII with the intracellular loop II of Na_v1.5 or control GST alone purified by GSH–Sepharose from *Escherichia coli* transformed with respective GST-plasmids. GST pull-down was then carried out, and MOG1 was detected using Western blot analysis with an anti-FLAG antibody. B, quantified data on the relative binding levels between WT MOG1, mutant MOG1, and Na_v1.5–LII from studies as in A. Error bars indicate S.D. (*n* = 3).

increasing sodium current density (Fig. 3, A–C). However, two deletion mutants, MOG1 (146–155 aa deletion) and MOG1 (136–145 aa deletion) failed to enhance sodium current density (Fig. 3, A–C). Consistent with the patch clamp data, mutants MOG1 (146–155 aa deletion) and MOG1 (136–145 aa deletion) failed to be pulled down by GST–Na_v1.5–LII, whereas the other three mutants, MOG1 (166–174 aa deletion), MOG1 (156–165 aa deletion), and MOG1 (126–135 aa deletion), were successfully pulled down by GST–Na_v1.5–LII (Fig. 4, A and B). Together, these data suggest that amino acid residues between 136 and 155 of MOG1 are involved in MOG1 interaction with Nav1.5–LII to increase sodium current density.

Point mutation analysis identifies critical amino acids of MOG1 required for Na_v1.5 function and enhancement of sodium current density

To determine the critical amino acid residues between 136 and 155 of MOG1 required for interaction with Na_v1.5–LII and for increasing sodium current density, alanine-scanning mutagenesis was performed for individual amino acid residues

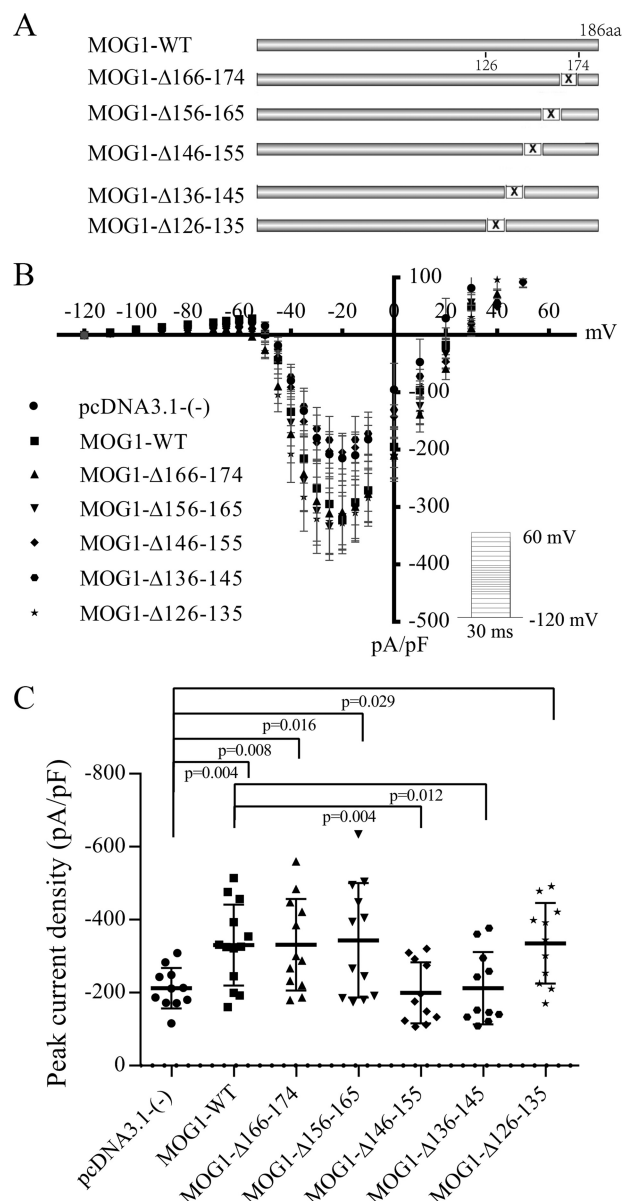


Figure 3. Microdeletion analysis of MOG1 for amino acid residues from 174 to 126 to identify the Na_v1.5 interaction domain. A, diagram showing WT MOG1 (*MOG1-WT*) and mutant MOG1 with five serial deletions from residues 174 to 126. B, effect of MOG1-WT and each deletion mutant on sodium current as compared with vector control pcDNA3.1(-). Error bars indicate S.E. C, peak sodium current density (pA/pF). The peak current density (pA/pF) was -212.56 ± 55.43 for pcDNA3.1(-) (11 cells), -330.30 ± 111.08 for MOG1-WT (13 cells), -331.01 ± 125.37 for MOG1-Δ166–174 (12 cells), -343.54 ± 156.59 for MOG1-Δ156–165 (12 cells), -199.49 ± 84.01 for MOG1-Δ146–155 (11 cells), -212.31 ± 98.83 for MOG1-Δ136–145 (11 cells), and -335.72 ± 165.29 for MOG1-Δ126–135 (11 cells). Values are mean \pm S.D.

in the region (Fig. 5A). Whole-cell patch clamp analysis showed that WT MOG1 increased sodium current density, but MOG1 mutants with mutations at L138A, L139A, D148A, R150A, or S151A failed to increase sodium current density (Fig. 5A). These data identified two MOG1 domains which impaired MOG1-mediated increase of cardiac sodium current density, region I at amino acid residues Leu-138 and Leu-139 and region II at amino acids Asp-148 to Ser-151. GST pull-down assays showed that GST–Na_v1.5–LII failed to pull down mutants MOG1 (L138A) and MOG1 (L139A) at region I (Fig. 5, B and

Defect of MOG1–Na_v1.5 interaction causes Brugada syndrome

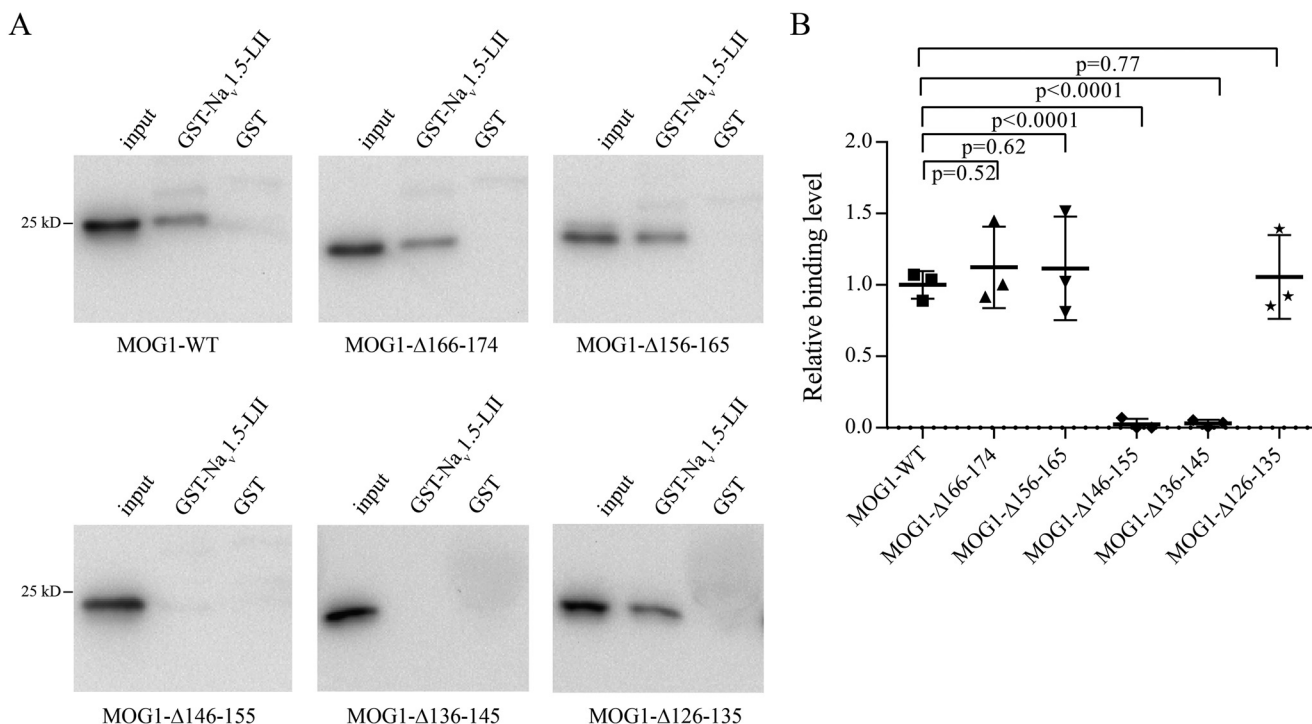


Figure 4. Interaction between WT and mutant MOG1 and each deletion mutant in a region from 126 to 174 and Na_v1.5. *A*, GST pull-down assays revealed that MOG1-Δ146–155 and MOG1-Δ136–145 failed to interact with GST–Na_v1.5–LII. MOG1-Δ166–174, MOG1-Δ156–165, and MOG1-Δ126–135 were successfully pulled down by GST–Na_v1.5–LII. *B*, quantified data on the relative binding levels between WT and mutant MOG1 and Na_v1.5–LII from studies as in *A*. Error bars indicate S.D. ($n = 3$).

C). The interaction between GST–Na_v1.5–LII and MOG1 mutants with mutations at D148A, R150A, or S151A at region II was also decreased compared with that with WT MOG1 (Fig. 5, *B* and *C*).

The overall effects of MOG1 alanine-scanning mutations at region I (L138A, L139A) were more dramatic than that of similar mutations at region II (D148A, R150A, S151A) (Fig. 5, *A–C*). To identify the underlying cause, we analyzed the affected amino acid residues against the 3D structure of MOG1 as reported by Bao *et al.* (15). As shown in Fig. 5*D*, Leu-138 and Leu-139 are located in the inner part of MOG1, consistent with their characteristics as amino acids with nonpolar side chains (Fig. 5*D*). Because they are buried inside the structure of MOG1, Leu-138 and Leu-139 cannot be the amino acid residues that interact directly with Na_v1.5. Thus, the effects of Leu-138A and Leu-139A could be because of structural changes of MOG1. Nevertheless, our data suggest that Leu-138 and Leu-139 may be involved in establishing the integrity of the MOG1 structure as their mutations to alanine may destabilize the overall structure of MOG1 so that the interaction between MOG1 and Na_v1.5 was disrupted.

Residues Asp-148, Arg-150, and Ser-151 of MOG1 are polar and charged amino acids located on the surface of the molecule (Fig. 5*D*). To further confirm their functional roles in MOG1, we constructed D148Q, R150Q, and S151Q mutations with more dramatic changes. Whole-cell patch clamp analysis showed that unlike WT MOG1, all three mutant MOG1 (D148Q, R150Q, S151Q) failed to increase cardiac sodium current density (Fig. 6, *A* and *B*). GST pull-down assays showed that these three mutant MOG1 failed to interact with GST–

Na_v1.5–LII (Fig. 6, *C* and *D*). These data suggest that amino acid residues Asp-148, Arg-150, and Ser-151 are the critical amino acids required for MOG1–Na_v1.5 interaction, which is required for increased I_{Na} density. We refer to the MOG1 region centered at Asp-148 to Ser-151 as the Na_v1.5 interaction domain of MOG1.

MOG1 increases cardiac sodium current density through facilitating Na_v1.5 trafficking to the plasma membrane. To determine the effects of the amino acid residues of the Na_v1.5 interaction domain on the plasma membrane expression level of Na_v1.5, mutant MOG1 with mutations L138A, L139A, D148Q, R150Q, or S151Q and pcDNA3–SCN5A were co-transfected into tsA201 cells. The biotinylated plasma membrane proteins were isolated and used for Western blot analysis to determine the expression level of Na_v1.5 in the plasma membrane. In contrast to WT MOG1, all five MOG1 mutants failed to increase the level of Na_v1.5 in the plasma membrane (Fig. 7, *A–D*). As a control, the Na_v1.5 expression level in total cell lysates was not affected by the five MOG1 mutants (Fig. 7, *A–D*).

Effect of Brugada syndrome mutation E83D of MOG1 on MOG1–Na_v1.5 interaction and sodium current density

A mutation in MOG1, E83D, was identified in a patient with BrS and significantly reduced the density of cardiac sodium current (18). However, the underlying molecular mechanism was poorly understood. Interestingly, our computer structural modeling analysis showed that the Glu-83 residue of MOG1 is located in close proximity to the Na_v1.5 interaction domain (Fig. 5*D*). Thus, we hypothesized that the Glu-83 residue of

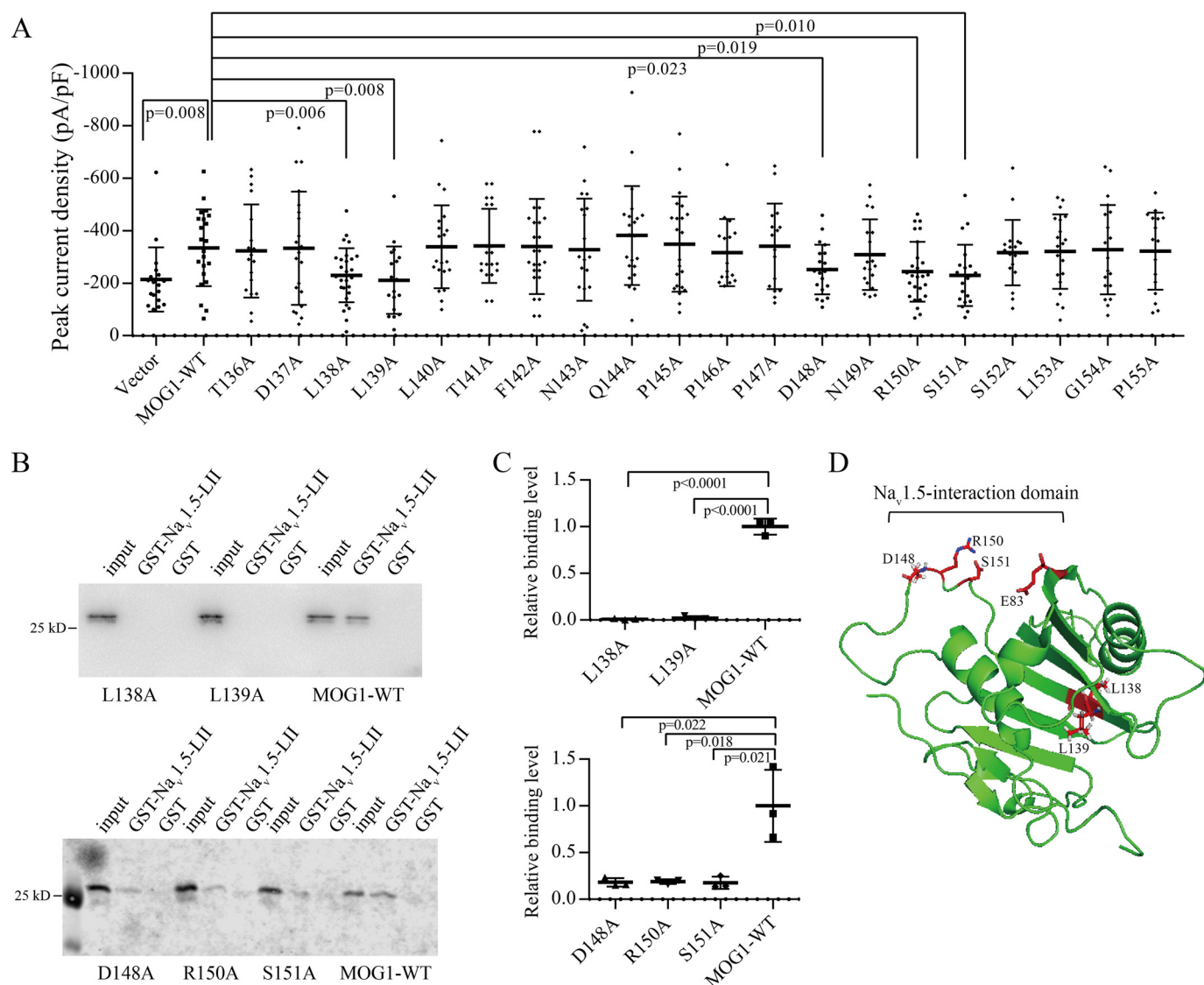


Figure 5. Identification of the critical amino acid residues for MOG1- $\text{Na}_v1.5$ function. Alanine-scanning mutagenesis was used to systematically mutate each amino acid residue between 136 and 155. *A*, effect of WT MOG1 (MOG1-WT) and each point mutation on the peak sodium current density. The peak current density (pA/pF) was -214.73 ± 122.06 for pcDNA3.1- (-) (18 cells), -335.46 ± 146.39 for MOG1-WT (22 cells), -323.56 ± 177.54 for T136A (18 cells), -339.94 ± 215.48 for D137A (21 cells), -231.09 ± 103.11 for L138A (26 cells), -211.92 ± 128.54 for L139A (18 cells), -339.44 ± 158.05 for L140A (21 cells), -342.86 ± 141.42 for T141A (20 cells), -340.58 ± 180.76 for F142A (24 cells), -328.57 ± 194.45 for N143A (20 cells), -382.30 ± 232.42 for Q144A (22 cells), -349.78 ± 180.99 for P145A (22 cells), -317.06 ± 128.00 for P146A (16 cells), -341.18 ± 162.71 for P147A (16 cells), -252.88 ± 94.36 for D148A (26 cells), -309.47 ± 134.74 for N149A (19 cells), -244.82 ± 113.98 for R150A (27 cells), -230.35 ± 116.52 for S151A (24 cells), -316.84 ± 124.46 for S152A (18 cells), -321.18 ± 141.01 for L153A (20 cells), -328.34 ± 170.50 for G154A (20 cells), and -322.94 ± 146.94 for P155A (17 cells). Values are mean \pm S.D. *B*, GST pull-down assays. MOG1 mutations L138A or L139A impaired the interaction between MOG1 and GST- $\text{Na}_v1.5$ -LII and failed to increase sodium current density. Mutations D148A, R150A, or S151A significantly decreased MOG1 interaction with GST- $\text{Na}_v1.5$ -LII and the peak sodium current density. *C*, quantified data on the relative binding levels between WT and mutant MOG1 and $\text{Na}_v1.5$ -LII from studies as in *B*. Error bars indicate S.D. ($n = 3$). *D*, diagram showing the location of residues Glu-83, Leu-138, Leu-139, Asp-148, Arg-150, Ser-151 in the structure of MOG1. The MOG1 structure was from Protein Data Bank (PDB ID: 5YFG).

MOG1 is also involved in the interaction between MOG1 and loop II of $\text{Na}_v1.5$, and that the E83D mutation of MOG1 disrupts the interaction between MOG1 and $\text{Na}_v1.5$, thus preventing MOG1 from facilitating $\text{Na}_v1.5$ trafficking to the cell surface. To test this hypothesis, we performed GST pull-down assays with mutant MOG1 with the E83D mutation. As shown in Fig. 8A, GST- $\text{Na}_v1.5$ -LII failed to pull down mutant MOG1 (E83D), although the positive control, WT MOG1, successfully pulled down GST- $\text{Na}_v1.5$ -LII. Moreover, we performed Western blot analysis with biotinylated plasma membrane proteins isolated from the cells co-transfected with pcDNA3-SCN5A and a WT FLAG-MOG1 plasmid, a mutant FLAG-E83D plas-

mid, or an empty vector control. Overexpression of WT MOG1 significantly increased the expression level of $\text{Na}_v1.5$ in the plasma membrane as compared with empty vector control, however, mutant MOG1 with the E83D mutation failed to increase $\text{Na}_v1.5$ in the plasma membrane as compared with WT MOG1 (Fig. 8, B and C). As a control, the $\text{Na}_v1.5$ expression level in total cell lysates was not affected by MOG1 mutation E83D (Fig. 8, B and C). These results suggest that the mechanism by which MOG1 mutation E83D causes BrS is that it disrupts the interaction between MOG1 and $\text{Na}_v1.5$, which significantly decreases the level of $\text{Na}_v1.5$ in the plasma membrane, resulting in reduced sodium current density.

Defect of *MOG1*-*Na_v1.5* interaction causes *Brugada syndrome*

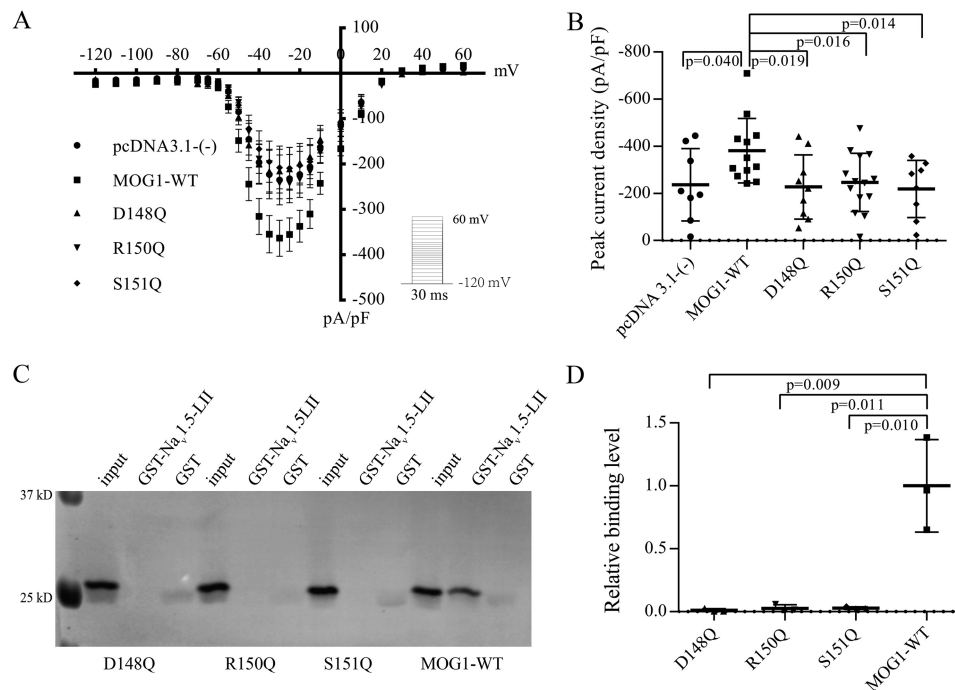


Figure 6. Amino acid residues Asp-148, Arg-150, and Ser-151 of *MOG1* are critical for interaction with *Na_v1.5* and for increasing sodium current density. Residues Asp-148, Arg-150, and Ser-151 were mutated to glutamine with a predicted larger effect than alanine. **A**, effect of WT *MOG1* and mutant D148Q, R150Q, or S151Q on sodium current density. **B**, effect of WT *MOG1* and mutant D148Q, R150Q, or S151Q on peak sodium current density. The peak current density (pA/pF) was -237.18 ± 153.35 for pcDNA3.1(-) (8 cells), -381.73 ± 136.76 for MOG1-WT (12 cells), -227.89 ± 136.40 for D148Q (9 cells), -246.88 ± 123.32 for R150Q (13 cells), and -219.10 ± 121.21 for S151Q (8 cells). Values are mean \pm S.D. **C**, GST pull-down assays for interaction between GST-*Na_v1.5-LII* and D148Q, R150Q, S151Q, and WT *MOG1*. **D**, quantified data on the relative binding levels between WT and mutant *MOG1* and *Na_v1.5-LII* from studies as in **C**. **Error bars indicate S.D.** ($n = 3$).

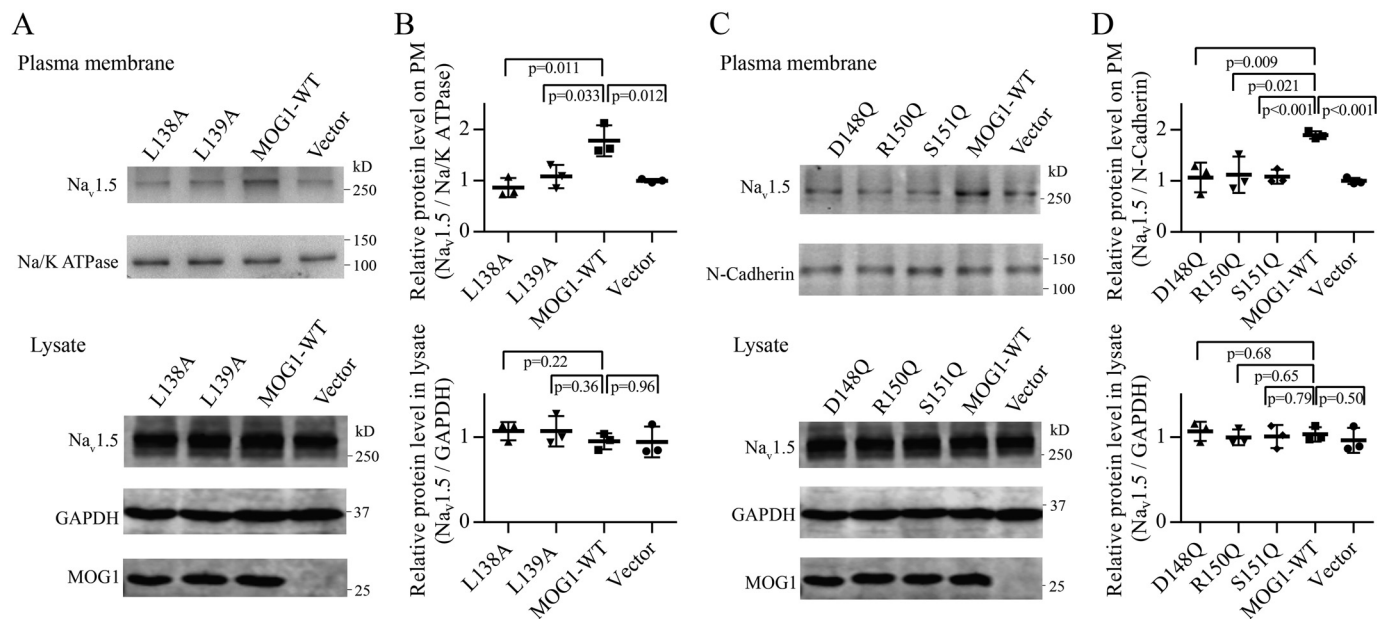


Figure 7. *MOG1* mutants L138A, L139A, D148Q, R150Q, and S151Q all failed to increase *Na_v1.5* expression in the plasma membrane (PM). **A** and **C**, Western blotting images of *Na_v1.5* in the plasma membranes and in the total lysates from HEK293 cells co-transfected with pcDNA-SCN5A and WT *MOG1* or mutant *MOG1*. **B** and **D**, quantification of plasma membrane (PM) and total protein expression levels of *Na_v1.5* in **A** and **C**, respectively. **Error bars indicate S.D.** ($n = 3$).

Similar effects between *MOG1* mutations D148Q, R150Q, and S151Q that disrupt binding to *Na_v1.5-LII* and E83D

To determine whether *MOG1* mutants D148Q, R150Q, S151Q, and E83D act in a dominant negative manner, we recorded sodium currents from the tsA201 cells co-transfected

with an *SCN5A* expression plasmid and an equal amount of WT *MOG1* and each mutant *MOG1* as compared with WT *MOG1* only. As shown in **Fig. 9, A and B**, the I_{Na} densities for overexpression of WT *MOG1* ($0.5 \mu\text{g WT} + 0.5 \mu\text{g vector}$) were significantly decreased by co-expression of each of the four

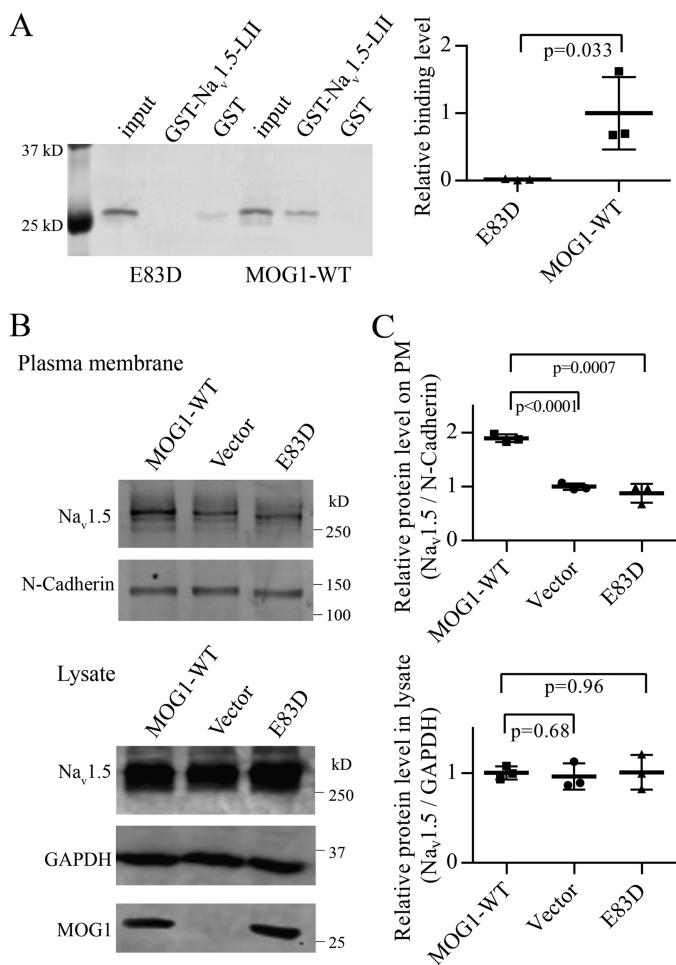


Figure 8. Brugada syndrome associated MOG1 mutation E83D disrupts the interaction between MOG1 and Na_v1.5 and reduces Na_v1.5 levels at cell surface. *A*, GST pull-down assays. GST–Na_v1.5–LII pulled WT MOG1 down, but not mutant MOG1 with mutation E83D. Error bars indicate S.D. ($n = 3$). *B*, Western blotting images showing Na_v1.5 expression levels in plasma membranes and total cell lysates. *C*, quantification of plasma membrane (PM) Na_v1.5 expression levels and total Na_v1.5 expression levels from images in *B*. Error bars indicate S.D. ($n = 3$).

mutant MOG1 (0.5 μ g WT + 0.5 μ g mutant MOG1). The data suggest that MOG1 mutants D148Q, R150Q, S151Q, and E83D all act in a dominant negative manner in reduction of I_{Na} densities. Consistent with the I_{Na} data, GST pull-down assays showed that the binding levels between WT MOG1 and Na_v1.5–LII were significantly decreased by co-expression of each of the four mutant MOG1 (Fig. 9, *C* and *D*).

Discussion

Mutations in Na_v1.5 cause an inherited arrhythmia of BrS (2), cardiac conduction disease (3), sick sinus syndrome (4), atrial fibrillation (5), dilated cardiomyopathy (5), and sudden infant death syndrome (6). The treatment options for BrS, cardiac conduction disease and sick sinus syndrome are highly limited except for implantation of implantable cardiac defibrillators and pacemakers. Approximately 50% of Na_v1.5 mutations are associated with significantly reduced cardiac sodium current density by blocking intracellular trafficking of Na_v1.5 to cell surface (20). Therefore, interventions that reverse the effects of Na_v1.5 on intracellular trafficking of Na_v1.5 to cell

surface was proposed as potential strategies to treat patients with BrS, cardiac conduction disease, and sick sinus syndrome (17). We previously showed that MOG1 significantly promoted intracellular trafficking of Na_v1.5 to cell surface and increased cardiac sodium current density (9). Moreover, MOG1 overexpression reversed the effects of trafficking-defective mutations D1275N and G1743R of Na_v1.5 on cell surface expression of Na_v1.5 and sodium current density (17). However, the molecular mechanism by which MOG1 promotes intracellular trafficking of Na_v1.5 to cell surface is poorly understood. Studies to identify how MOG1 interacts with Na_v1.5 are important for understanding the role of MOG1 in intracellular trafficking of Na_v1.5. In this study, we defined the functional domain and precise amino acid residues of MOG1 that are required for its interaction with Na_v1.5. By analyzing the interaction of the intracellular loop II of Na_v1.5 with WT MOG1 and eight serial deletion mutants of MOG1 and characterizing the effects of deletions on cardiac sodium current density, we defined the Na_v1.5–interaction domain of MOG1 between amino acid residue Thr-136 and Pro-155 (Figs. 1–3). Similar analysis but with alanine-scanning mutations identified the specific amino acid residues of MOG1 that are essential for MOG1–Na_v1.5 interaction, including Asp-148, Arg-150, and Ser-151. These three amino acid residues are located in an extended outside α -helix loop on the surface of the MOG1 structure (Fig. 5*D*), which is best suited for contacting Na_v1.5.

Interestingly, our deletion and alanine-scanning mutation analyses revealed only one half of the Na_v1.5 interaction domain of MOG1. The other half was identified in an interesting manner. Our computer modeling analysis revealed that the Glu-83 residue of MOG1 is located in a close proximity in the 3D structure of MOG1 (Fig. 5*D*). Functional studies showed that mutation E83D, which is associated with Brugada syndrome, disrupted the interaction between MOG1 and Na_v1.5 (Fig. 8), suggesting that the Glu-83 residue is also involved in the interaction between MOG1 and Na_v1.5. The Glu-83 residue is located in nearby α -helix loop on the surface of the MOG1 structure (Fig. 5*D*). Overall, the α -helix loop at Asp-148 to Ser-151 and the α -helix loop at Glu-83 form the two separate sides of a clamp, respectively, which may make MOG1 bind to Na_v1.5 by clamping down on a specific structure of Na_v1.5 (Fig. 5*D*). Interestingly, Asp-148, Arg-150, and Glu-83 are all charged amino acid residues, which may interact with Na_v1.5 amino acid residues with opposite charges.

During our alanine-scanning mutation analysis, we identified two amino acid residues, Leu-138 and Leu-139, that appeared to disrupt the interaction between MOG1 and Na_v1.5 and reduce cardiac sodium current density (Fig. 5, *A–C*). However, Leu-138 and Leu-139 are nonpolar amino acid residues and computer modeling analysis of the MOG1 structure revealed that these two residues are buried inside the MOG1 structure (Fig. 5*D*). As such, it is impossible for Leu-138 and Leu-139 of MOG1 to make direct contact with Na_v1.5. Instead, Leu-138 and Leu-139 may be essential for maintaining the overall structure of MOG1 so that when either one is mutated to alanine, the overall structure of MOG1 is altered, which disrupts the interaction between MOG1 and Na_v1.5 and reduces cardiac sodium current density.

Defect of *MOG1*-*Na_v1.5* interaction causes Brugada syndrome

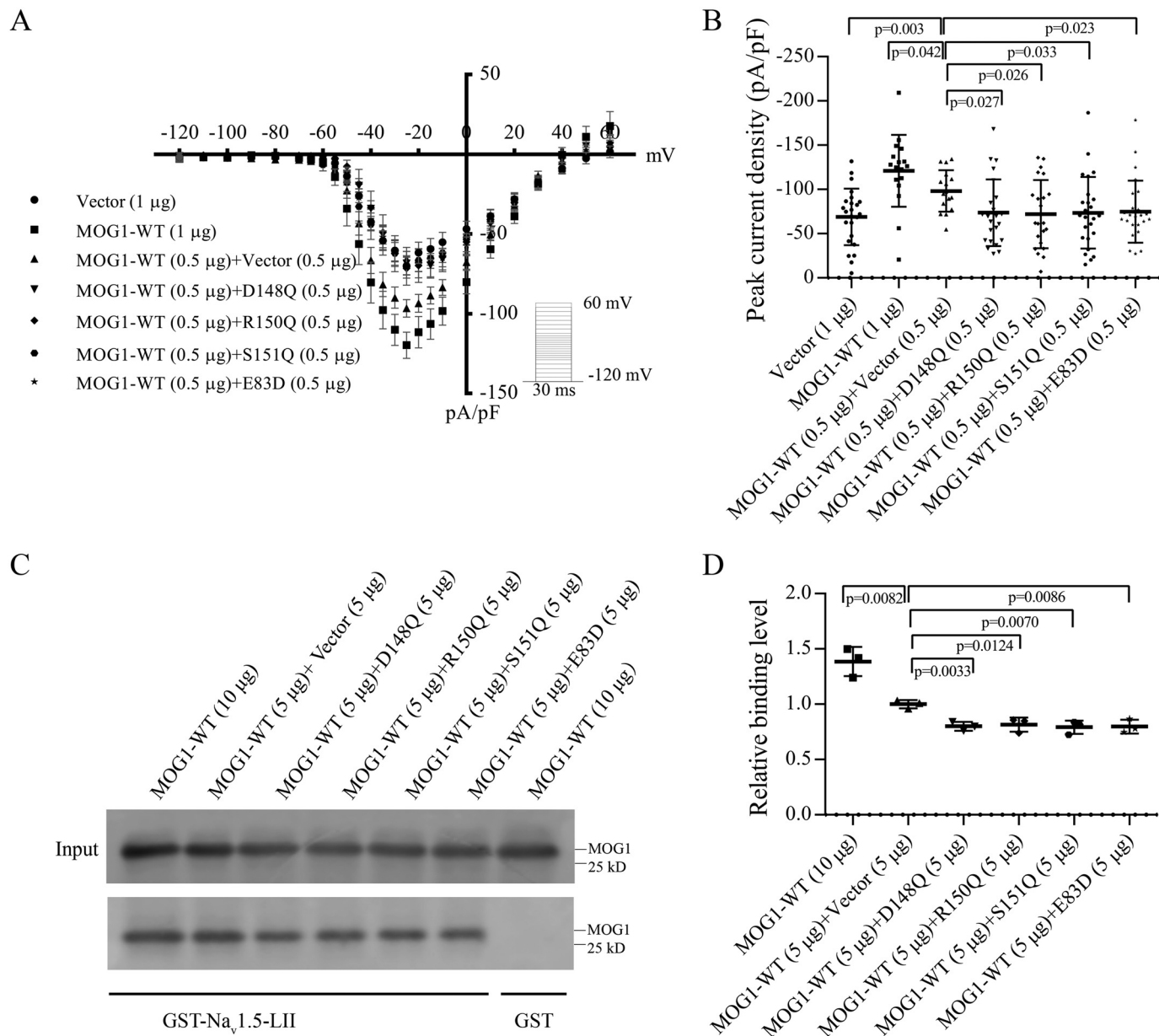


Figure 9. *MOG1* mutations D148Q, R150Q, and S151Q that disrupt the interaction between *MOG1* and *Na_v1.5* act in a dominant negative manner as Brugada syndrome mutation E83D. *A*, effects of *MOG1* mutations E83D, D148Q, R150Q, and S151Q on sodium current densities in tsA201 cells co-transfected with 0.2 μ g of pcDNA3-SCN5A and an equal amount of WT *MOG1* (*MOG1*-WT). The empty vector (1 μ g) was used as a negative control, and *MOG1*-WT (1 μ g) and *MOG1*-WT (0.5 μ g) + vector (0.5 μ g) were used as positive controls. *Error bars* indicate S.E. *B*, the peak sodium current densities (pA/pF) derived from *A*: -68.93 ± 32.05 for vector pcDNA3.1- (-) (24 cells), -124.14 ± 43.46 for *MOG1*-WT (1 μ g) (17 cells), -98.20 ± 23.43 for *MOG1*-WT (0.5 μ g) + vector (0.5 μ g) (16 cells), -73.62 ± 37.79 for *MOG1*-WT (0.5 μ g) + D148Q (0.5 μ g) (23 cells), -72.06 ± 40.67 for *MOG1*-WT (0.5 μ g) + R150Q (0.5 μ g) (22 cells), -73.59 ± 40.41 for *MOG1*-WT (0.5 μ g) + Ser-151 (0.5 μ g) (25 cells), and -74.77 ± 35.14 for *MOG1*-WT (0.5 μ g) + E83D (0.5 μ g) (25 cells). Values are mean \pm S.D. *C*, GST pull-down assays for interaction between GST-*Na_v1.5*-LII and WT *MOG1*, and an equal amount of WT *MOG1* and each mutant *MOG1* (D148Q, R150Q, S151Q, or E83D). Note that more DNA was needed for transfection for GST pull-down assays than for *I_{Na}* recording. *D*, quantified data from Western blot analysis as in (*C*) for the relative binding levels between GST-*Na_v1.5*-LII and WT *MOG1*, and WT/mutants. *Error bars* indicate S.D. ($n = 3$).

We reported previously that *SCN5A* is the first gene responsible for Brugada syndrome (2). As *MOG1* interacts with and regulates the function of the cardiac sodium channel encoded by *SCN5A* (9), *MOG1* became a candidate gene for Brugada syndrome. Kattynarath *et al.* (18) later reported a dominant negative mutation in *MOG1*, E83D, in a patient with Brugada syndrome. Overexpression of mutant E83D or E83D + WT in HEK *Na_v1.5* stable cells failed to increase cardiac sodium current density. However, the molecular mechanism was poorly understood. In this study, we show that the E83D mutation of

MOG1 disrupts the interaction between *MOG1* and *Na_v1.5* and reduces intracellular trafficking of *Na_v1.5* to cell surface (Fig. 8). Our data provide a mechanistic understanding of why *MOG1* mutation E83D significantly reduces cardiac sodium current density, and thereby uncovers a novel molecular mechanism for the pathogenesis of Brugada syndrome. It is interesting to note that a mutation from a glutamic acid residue (E) to an aspartic acid (D) is considered to be a minor change because the mutation does not change the overall negative charge, but simply reduces a methylene bridge ($-\text{CH}_2-$) on the side chain.

However, our finding that the E83D mutation is located in the MOG1–Na_v1.5 interaction domain explains why such a weak mutation has a dramatic effect to cause a human disease because a deletion of one methylene bridge (–CH₂–) in the MOG1–Na_v1.5 interaction pocket can make the interaction weakened, thereby disrupting the interaction and causing a dramatic functional effect.

The data from both patch clamp recordings of I_{Na} and GST pulldown assays for the interaction between Na_v1.5–LII and MOG1 suggest that MOG1 mutations D148Q, R150Q, and R151Q as well as mutation E83D associated with Brugada syndrome act in a dominant negative manner to antagonize the functional effects of WT MOG1 (Fig. 9). 3D structural studies suggest that MOG1 is a monomer (15). How does the mutant MOG1 interfere with the function of WT MOG1 to exert the dominant negative effect? One possibility is that MOG1 may function as a dimer or multimer *in vivo*, and mutant MOG1 binds to WT MOG1 to disrupt its binding to Na_v1.5 and reduce I_{Na} densities. An alternative possibility may be related to the finding that MOG1 is an adaptor protein that can interact with other proteins. MOG1 was shown to interact with Ran GTPase (10, 11). We recently found that small GTPases SAR1A and SAR1B interacted with MOG1, and the interaction was involved in MOG1-mediated cell surface expression and function of Na_v1.5 (26). Therefore, mutant MOG1 may interfere with the interaction between WT MOG1 and SAR1 or other proteins that are in the complex with Na_v1.5 and required for trafficking of Na_v1.5, resulting in reduced I_{Na} densities. These and other hypotheses can be tested in the future to further define the detailed molecular mechanism(s) underlying the dominant negative effect of MOG1 mutations.

A limitation of this study is that all experiments were performed in HEK293 cells. We have reported that the functional effects of MOG1 on Na_v1.5 and cardiac sodium currents in HEK293 cells are similar to those found in isolated neonatal cardiomyocytes (9, 17). Moreover, Kattynarath *et al.* (18) reported that mutation E83D associated with Brugada syndrome showed a similar effect in HEK293 cells and adult rat atrial cardiomyocytes. Therefore, it is possible that the findings on MOG1 and MOG1 mutations in HEK293 cells may be extended to cardiac myocytes. However, future studies using isolated neonatal cardiomyocytes are needed to test this possibility.

In summary, the data in this study identify the Na_v1.5 interaction domain of MOG1, and define the MOG1–Nav1.5 interaction domain as a potential clamp structure with the α -helix loop at Asp-148 to Ser-151 as one side of the clamp and the α -helix loop at Glu-83 as the other side of the clamp. Our data also identify important structural elements, including several charged amino acid residues, Asp-148, Arg-150, and Glu-83, which are essential for the interaction between MOG1 and Na_v1.5, and may make direct contact with Na_v1.5 amino acid residues with opposite charges. Moreover, we uncovered a possible molecular mechanism by which MOG1 mutation E83D causes Brugada syndrome. The identification of the MOG1 domain required for full Na_v1.5 function may facilitate rational design of agents to rescue the trafficking defects of Na_v1.5 mutations associated with Brugada syndrome, sick sinus syn-

drome, atrial fibrillation, dilated cardiomyopathy, common heart failure, and myocardial ischemia.

Experimental procedures

Plasmids

WT and mutant MOG1 expression plasmids for electrophysiological analysis in mammalian cells were constructed using the pcDNA3.1- (–) vector. The PCR primers used for amplification of MOG1 cDNA include the forward primer with an EcoR I restriction enzyme site, 5'-ATTTCGAATTCGCCAC-CATGGAGCCCACGAGAGACT-3' and the reverse primer with a BamH I restriction site, 5'-CGATGGATCCTTACTGGG GACCAAGATG-3'. MOG1 deletions were made using overlapping PCR analysis. Alanine-scanning mutations were also created using overlapping PCR-based mutagenesis. The WT and mutant MOG1 expression plasmids for GST pulldown assays were constructed using the p3×FLAG CMV10 vector. The PCR primers used for amplification of MOG1 cDNA include the forward primer with a HindIII restriction enzyme site, 5'-GACCAAGCTTATGGAGCCCACGAGAGAC-3' and the reverse primer with an EcoR I restriction site, 5'-TTGCGAATTCCTTTTACTGGG GACCAAGAT-3'. The expression plasmid for GST–Na_v1.5–loop II (amino acids 940–1200) was cloned into pGEX-4T1 as described previously (9). The mammalian expression plasmid for SCN5A/Na_v1.5 is pcDNA3-SCN5A (pHL3) as described previously (2, 21).

Cell culture and transfection

The tsA201 cells were cultured and maintained in Dulbecco's modified Eagle's medium (DMEM, Gibco) supplemented with 10% (v/v) fetal bovine serum (FBS). A stable HEK293 cell line with constant expression of Na_v1.5, Na_v1.5/HEK, was cultured in DMEM (Gibco) with 10% (v/v) FBS and 50 μ g/ μ l of G418. For patch clamping recording, Na_v1.5/HEK cells were cultured on coverslips in 24-well plates to 80% confluence, and transiently transfected using GenJet (SignaGen Laboratories). The amount of plasmid DNA for each 24-well plate well was 0.8 μ g of WT, mutant MOG1, or empty vector pcDNA3.1- (–) as negative control, and 0.2 μ g of pmxEGFP as a transfection indicator. For GST pulldown assays, tsA201 cells were cultured in 10-cm dishes, and transfected with 10 μ g of plasmids with FLAG-tagged WT or mutant MOG1.

Electrophysiological analysis

The transfected Na_v1.5/HEK cells with an approximately equal amount of GFP signal were selected for whole cell voltage clamping recording of sodium current. Electrode resistance ranged from 2 to 4 megohms when filled with the pipette solution (20 mM NaCl, 130 mM CsCl, 10 mM HEPES, 10 mM EGTA, pH 7.2, with CsOH). The composition of bath solution was 70 mM NaCl, 80 mM CsCl, 5.4 mM KCl, 2 mM CaCl₂, 1 mM MgCl₂, 10 mM HEPES, 10 mM glucose, pH 7.3 with CsOH as described previously (9, 22, 23). Command pulses were generated using a MultiClamp 700B Amplifier (Axon Instruments) under the control of pCLAMP 10 software. The signals were digitized with a Digidata 1440A (Molecular Devices). Data were analyzed with Clampfit software.

Defect of MOG1–Na_v1.5 interaction causes Brugada syndrome

Isolation and characterization of plasma membranes proteins

The tsA201 cells were co-transfected with expression plasmids for Na_v1.5 (pcDNA3-SCN5A) and WT or mutant FLAG-tagged MOG1. Proteins on plasma membranes were biotinylated using the EZ-Link Sulfo-NHS-SS-Biotin kit (Pierce) according to the manufacturer's instructions. The cells were then lysed in TNEN buffer (50 mM Tris/HCl, pH 7.5, 150 mM NaCl, 2.0 mM EDTA, 1% Nonidet P-40), and biotinylated proteins were captured using Pierce™ UltraLink™ Immobilized NeutrAvidin™ Resin as described previously (9, 17). Western blot analysis was then performed using an anti-Na_v1.5 antibody or other control antibodies as described previously (9).

GST pulldown assays

The tsA201 cells were transfected with plasmids for FLAG-tagged MOG1 and lysed in TNEN lysis buffer. GST-tagged Na_v1.5–loop II (GST–Na_v1.5–LII) was expressed in BL21 cells induced by IPTG (isopropyl β-D-thiogalactopyranoside) at 26 °C for 8 h. GST-tagged Na_v1.5 loop II (amino acids 940–1200) was used as bait to capture WT or mutant FLAG-MOG1 as described by us previously (9). GSH Sepharose 4B beads (GE Healthcare) were used to bind GST–Na_v1.5–LII or GST alone as negative control. The products pulled down by GST were analyzed by Western blot analysis using an anti-FLAG antibody (Sigma).

Western blot analysis

Western blot analysis was performed as described previously (24, 25). For Western blot analysis for Na_v1.5, we used 8% gels for separating proteins, whereas for MOG1, we used 15% gels. Primary antibodies used for Western blot analysis are those for FLAG (Sigma, F1804, F3165, 1:2000 dilution), Na_v1.5 (Protein-tech Group, 23016-A-P, 1:1000; Alomone Labs, ASC-005, ASC-013, 1:1000 dilution), Na/K ATPase (Sigma, 06-520, 1:1000 dilution), and N-cadherin (Novus Biologicals, NB200-592, 1:500 dilution). The secondary antibodies are goat anti-mouse HRP-conjugated secondary antibody (Millipore, 1:20,000), goat anti-rabbit HRP-conjugated secondary antibody (Millipore, 1:20,000), goat anti-mouse IRDye 680LT (LI-COR Biosciences, 926-68020, 1:20,000), or goat anti-rabbit IRDye 800CW (LI-COR, 926-32111, 1:20000). The intensity of each band from Western blot images was quantified and analyzed by Quantity One analysis software 4.6.2 version (Bio-Rad Laboratories) or Image Studio (LI-COR).

Statistical analysis

Quantitative data were presented as mean ± S.E. for sodium channel current-voltage characteristics and mean ± S.D. for others. The difference between two groups was analyzed by a Student's *t* test. A *p* value of < 0.05 was considered to be statistically significant.

Author contributions—G. Y. data curation; G. Y. software; G. Y., J. Q., Q. C., and Q. K. W. formal analysis; G. Y., Y. Liu, Z. W., Y. H., F. W., Y. Li, and S. C. investigation; G. Y. and Y. Liu methodology; G. Y. writing-original draft; Y. Liu validation; J. Q., Q. C., and Q. K. W. conceptualization; J. Q., Q. C., and Q. K. W. writing-review and editing; Q. C. and Q. K. W. resources; Q. C. and Q. K. W. project administration; Q. K. W. and Q. C. supervision; Q. K. W. and Q. C. funding acquisition.

Acknowledgments—We thank Dr. Charles Antzelevitch for the tsA201 cell line and Dr. Glenn Kirsch for Na_v1.5/HEK stable expression cell line.

References

1. Willich, S. N., Levy, D., Rocco, M. B., Tofler, G. H., Stone, P. H., and Muller, J. E. (1987) Circadian variation in the incidence of sudden cardiac death in the Framingham Heart Study population. *Am. J. Cardiol.* **60**, 801–806 [CrossRef Medline](#)
2. Chen, Q., Kirsch, G. E., Zhang, D., Brugada, R., Brugada, J., Brugada, P., Potenza, D., Moya, A., Borggrefe, M., Breithardt, G., Ortiz-Lopez, R., Wang, Z., Antzelevitch, C., O'Brien, R. E., Schulze-Bahr, E., Keating, M. T., Towbin, J. A., and Wang, Q. (1998) Genetic basis and molecular mechanism for idiopathic ventricular fibrillation. *Nature* **392**, 293–296 [CrossRef Medline](#)
3. Schott, J. J., Alshinawi, C., Kyndt, F., Probst, V., Hoorntje, T. M., Hulsbeek, M., Wilde, A. A., Escande, D., Mannens, M. M., and Le Marec, H. (1999) Cardiac conduction defects associate with mutations in SCN5A. *Nat. Genet.* **23**, 20–21 [CrossRef Medline](#)
4. Benson, D. W., Silberbach, G. M., Kavanaugh-McHugh, A., Cottrill, C., Zhang, Y., Riggs, S., Smalls, O., Johnson, M. C., Watson, M. S., Seidman, J. G., Seidman, C. E., Plowden, J., and Kugler, J. D. (1999) Mutations in the cardiac transcription factor NKX2.5 affect diverse cardiac developmental pathways. *J. Clin. Invest.* **104**, 1567–1573 [CrossRef Medline](#)
5. Olson, T. M., Michels, V. V., Ballew, J. D., Reyna, S. P., Karst, M. L., Herron, K. J., Horton, S. C., Rodeheffer, R. J., and Anderson, J. L. (2005) Sodium channel mutations and susceptibility to heart failure and atrial fibrillation. *JAMA* **293**, 447–454 [CrossRef Medline](#)
6. Otagiri, T., Kijima, K., Osawa, M., Ishii, K., Makita, N., Matoba, R., Umetsu, K., and Hayasaka, K. (2008) Cardiac ion channel gene mutations in sudden infant death syndrome. *Pediatr. Res.* **64**, 482–487 [CrossRef Medline](#)
7. Gellens, M. E., George, A. L., Jr., Chen, L. Q., Chahine, M., Horn, R., Barchi, R. L., and Kallen, R. G. (1992) Primary structure and functional expression of the human cardiac tetrodotoxin-insensitive voltage-dependent sodium channel. *Proc. Natl. Acad. Sci. U.S.A.* **89**, 554–558 [CrossRef Medline](#)
8. Wang, Q., Li, Z., Shen, J., and Keating, M. T. (1996) Genomic organization of the human SCN5A gene encoding the cardiac sodium channel. *Genomics* **34**, 9–16 [CrossRef Medline](#)
9. Wu, L., Yong, S. L., Fan, C., Ni, Y., Yoo, S., Zhang, T., Zhang, X., Obejero-Paz, C. A., Rho, H. J., Ke, T., Szafranski, P., Jones, S. W., Chen, Q., and Wang, Q. K. (2008) Identification of a new co-factor, MOG1, required for the full function of cardiac sodium channel Na_v1.5. *J. Biol. Chem.* **283**, 6968–6978 [CrossRef Medline](#)
10. Oki, M., and Nishimoto, T. (1998) A protein required for nuclear-protein import, Mog1p, directly interacts with GTP-Gsp1p, the *Saccharomyces cerevisiae* ran homologue. *Proc. Natl. Acad. Sci. U.S.A.* **95**, 15388–15393 [CrossRef Medline](#)
11. Steggerda, S. M., and Paschal, B. M. (2000) The mammalian Mog1 protein is a guanine nucleotide release factor for Ran. *J. Biol. Chem.* **275**, 23175–23180 [CrossRef Medline](#)
12. Baker, R. P., Harreman, M. T., Eccleston, J. F., Corbett, A. H., and Stewart, M. (2001) Interaction between Ran and Mog1 is required for efficient nuclear protein import. *J. Biol. Chem.* **276**, 41255–41262 [CrossRef Medline](#)
13. Stewart, M., and Baker, R. P. (2000) 1.9 Å resolution crystal structure of the *Saccharomyces cerevisiae* Ran-binding protein Mog1p. *J. Mol. Biol.* **299**, 213–223 [CrossRef Medline](#)
14. Baker, R. P., and Stewart, M. (2000) Crystallization and preliminary X-ray diffraction analysis of the *Saccharomyces cerevisiae* ran-binding protein Mog1p. *Acta Crystallogr. D. Biol. Crystallogr.* **56**, 229–231 [CrossRef Medline](#)
15. Bao, X., Liu, H., Liu, X., Ruan, K., Zhang, Y., Zhang, Z., Hu, Q., Liu, Y., Akram, S., Zhang, J., Gong, Q., Wang, W., Yuan, X., Li, J., Zhao, L., Dou, Z., Tian, R., Yao, X., Wu, J., and Shi, Y. (2018) Mitosis-specific acetylation

- tunes Ran effector binding for chromosome segregation. *J. Mol. Cell. Biol.* **10**, 18–32 [CrossRef Medline](#)
16. Steggerda, S. M., and Paschal, B. M. (2001) Identification of a conserved loop in Mog1 that releases GTP from Ran. *Traffic* **2**, 804–811 [CrossRef Medline](#)
 17. Chakrabarti, S., Wu, X., Yang, Z., Wu, L., Yong, S. L., Zhang, C., Hu, K., Wang, Q. K., and Chen, Q. (2013) MOG1 rescues defective trafficking of Na (v) 1.5 mutations in Brugada syndrome and sick sinus syndrome. *Circ. Arrhythm. Electrophysiol.* **6**, 392–401 [CrossRef Medline](#)
 18. Kattynarath, D., Maugenre, S., Neyroud, N., Balse, E., Ichai, C., Denjoy, I., Dilanian, G., Martins, R. P., Fressart, V., Berthet, M., Schott, J. J., Leenhardt, A., Probst, V., Le Marec, H., Hainque, B., Coulombe, A., Hatem, S. N., and Guicheney, P. (2011) MOG1: A new susceptibility gene for Brugada syndrome. *Circ. Cardiovasc. Genet.* **4**, 261–268 [CrossRef Medline](#)
 19. Marfatia, K. A., Harreman, M. T., Fanara, P., Vertino, P. M., and Corbett, A. H. (2001) Identification and characterization of the human MOG1 gene. *Gene* **266**, 45–56 [CrossRef Medline](#)
 20. Gui, J., Wang, T., Jones, R. P., Trump, D., Zimmer, T., and Lei, M. (2010) Multiple loss-of-function mechanisms contribute to SCN5A-related familial sick sinus syndrome. *PLoS One* **5**, e10985 [CrossRef Medline](#)
 21. Wang, Q., Shen, J., Splawski, I., Atkinson, D., Li, Z., Robinson, J. L., Moss, A. J., Towbin, J. A., and Keating, M. T. (1995) SCN5A mutations associated with an inherited cardiac arrhythmia, long QT syndrome. *Cell* **80**, 805–811 [CrossRef Medline](#)
 22. Tian, X. L., Yong, S. L., Wan, X., Wu, L., Chung, M. K., Tchou, P. J., Rosenbaum, D. S., Van Wagoner, D. R., Kirsch, G. E., and Wang, Q. (2004) Mechanisms by which SCN5A mutation N1325S causes cardiac arrhythmias and sudden death *in vivo*. *Cardiovasc. Res.* **61**, 256–267 [CrossRef Medline](#)
 23. Yong, S. L., Ni, Y., Zhang, T., Tester, D. J., Ackerman, M. J., and Wang, Q. K. (2007) Characterization of the cardiac sodium channel SCN5A mutation, N1325S, in single murine ventricular myocytes. *Biochem. Biophys. Res. Commun.* **352**, 378–383 [CrossRef Medline](#)
 24. Zhang, T., Yong, S. L., Tian, X. L., and Wang, Q. K. (2007) Cardiac-specific overexpression of SCN5A gene leads to shorter P wave duration and PR interval in transgenic mice. *Biochem. Biophys. Res. Commun.* **355**, 444–450 [CrossRef Medline](#)
 25. Tian, X. L., Kadaba, R., You, S. A., Liu, M., Timur, A. A., Yang, L., Chen, Q., Szafranski, P., Rao, S., Wu, L., Housman, D. E., DiCorleto, P. E., Driscoll, D. J., Borrow, J., and Wang, Q. (2004) Identification of an angiogenic factor that when mutated causes susceptibility to Klippel-Trenaunay syndrome. *Nature* **427**, 640–645 [CrossRef Medline](#)
 26. Wang, Z., Yu, G., Liu, Y., Liu, S., Aridor, M., Huang, Y., Hu, Y., Wang, L., Li, S., Xiong, H., Tang, B., Li, X., Cheng, C., Chakrabarti, S., Wang, F., et al. (2018) Small GTPases SAR1A and SAR1B regulate the trafficking of the cardiac sodium channel Nav1.5. *Biochim. Biophys. Acta. Mol. Basis Dis.* **1864**, 3672–3684 [CrossRef Medline](#)